

Charge injection and transport in single-layer organic light-emitting diodes

B. K. Crone, I. H. Campbell, P. S. Davids, and D. L. Smith

Citation: *Appl. Phys. Lett.* **73**, 3162 (1998); doi: 10.1063/1.122706

View online: <http://dx.doi.org/10.1063/1.122706>

View Table of Contents: <http://apl.aip.org/resource/1/APPLAB/v73/i21>

Published by the [American Institute of Physics](#).

Related Articles

Study of field driven electroluminescence in colloidal quantum dot solids

J. Appl. Phys. **111**, 113701 (2012)

Annealed InGaN green light-emitting diodes with graphene transparent conductive electrodes

J. Appl. Phys. **111**, 114501 (2012)

Noniterative algorithm for improving the accuracy of a multicolor-light-emitting-diode-based colorimeter

Rev. Sci. Instrum. **83**, 053115 (2012)

Effects of lateral current injection in GaN multi-quantum well light-emitting diodes

J. Appl. Phys. **111**, 103120 (2012)

Correlation between defect properties and internal quantum efficiency in blue-emitting InGaN based light emitting diodes

J. Appl. Phys. **111**, 103115 (2012)

Additional information on *Appl. Phys. Lett.*

Journal Homepage: <http://apl.aip.org/>

Journal Information: http://apl.aip.org/about/about_the_journal

Top downloads: http://apl.aip.org/features/most_downloaded

Information for Authors: <http://apl.aip.org/authors>

ADVERTISEMENT

The advertisement features a green and white background with abstract, flowing lines. At the top, the 'AIP Advances' logo is displayed, with 'AIP' in blue and 'Advances' in green. Below the logo, the text 'Special Topic Section: PHYSICS OF CANCER' is written in white. Underneath, the phrase 'Why cancer? Why physics?' is written in green. A blue button with white text 'View Articles Now' is located at the bottom right of the advertisement.

AIP Advances

Special Topic Section:
PHYSICS OF CANCER

Why cancer? Why physics? [View Articles Now](#)

Charge injection and transport in single-layer organic light-emitting diodes

B. K. Crone,^{a)} I. H. Campbell, P. S. Davids,^{b)} and D. L. Smith
Los Alamos National Laboratory, Los Alamos, New Mexico 87545

(Received 6 July 1998; accepted for publication 21 September 1998)

We present experimental and device model results for the current–voltage characteristics of a series of organic diodes. We consider three general types of structures: electron only, hole only, and bipolar devices. Electron and hole mobility parameters are extracted from the corresponding single carrier structures and then used to describe the bipolar devices. The device model successfully describes the experimental results for: electron only devices as thickness is varied, hole only devices as the contact metals are varied, and bipolar devices as both the thickness and the contact metals are varied. © 1998 American Institute of Physics. [S0003-6951(98)00547-6]

There is much interest in light-emitting diodes (LEDs) based on conjugated organic materials for large-area electronic applications, such as displays, due to their promise of low cost, easy processing, and low-temperature deposition over flexible or curved substrates.¹ A great deal of work has been done towards an understanding of the device physics of organic LEDs.^{1–6} Single-layer poly(dialkoxy-p-phenylene vinylene) LEDs have been systematically investigated.^{3,4} The electron and hole currents were studied in single carrier structures where the current was space-charge limited and not determined by the properties of the contacts.⁴ The recombination process was studied in bipolar devices employing space-charge-limited contacts and reported to be of the Langevin type.³

The device current of organic light-emitting diodes is determined by the injection, transport, and recombination of charge carriers. Charge injection depends on the Schottky energy barrier between the contact and the organic material. Charge transport and recombination depend on the material properties of the organic film. We consider structures where the injection processes at the contacts, the transport properties of carriers in the organic film, and the carrier recombination processes can be separated to as large a degree as possible. We present results for current–voltage characteristics of single organic layer LEDs consisting of metal_A/MEH–PPV/metal_B (denoted metal_A/metal_B) structures where MEH–PPV stands for poly[2-methoxy,5-(2'-ethyl-hexyloxy)–1,4-phenylene vinylene]. We select the contact metals of the devices so that either electrons or holes dominate the current flow. We use the results of these single carrier structures to separately determine the mobility parameters of the two carrier types. We then select the contact metals so that both electrons and holes are injected and use the single carrier mobility parameters to describe the measured current–voltage characteristics of the bipolar devices.

Carrier transport in organic films can be studied in a relatively simple situation by considering single organic layer structures in which the contacts are selected to provide space-charge-limited current for one carrier type and prevent efficient injection of the other carrier type. The current is

then due to the space-charge-limited current of one carrier and depends only on the bulk transport properties of the organic film for that carrier. Carrier injection can be studied in a relatively simple situation by considering a series of single organic layer structures in which only one contact efficiently injects carriers and the Schottky energy barrier to charge injection of that contact is varied by changing the contacting metal. Carrier recombination affects the injected carrier density, and hence, the I – V characteristics of bipolar devices. Carrier recombination also determines the luminance efficiencies of devices, however, quantitative evaluation in single-layer devices is complicated by cavity effects, dipole quenching near the electrodes, and extrinsic nonradiative recombination centers, and is the topic of future studies.⁷

We first consider Ca/Ca electron-only structures as a function of polymer thickness. Calcium provides a space-charge-limited electron contact. We describe the measured I – V characteristics with a device model and extract the electron mobility. For hole injecting structures in MEH–PPV, the device behavior can be varied from space-charge-limited current for small energy barrier contacts such as gold and platinum, to contact-limited current for large energy barrier contacts such as copper or aluminum.⁸ We consider Au/Al and Cu/Al hole-only devices. The holes are injected from the gold or copper contacts. We use previously determined Schottky energy barriers for these contacts to MEH–PPV, describe the measured I – V characteristics using a device model and extract the hole mobility. Finally, we consider Pt/Ca and Cu/Ca bipolar devices. Using the mobility parameters determined from the electron-only and the hole-only structures, the device model successfully describes the measured I – V curves for these bipolar devices with different thicknesses and injection barriers without additional fitting parameters.

The device model, described in detail elsewhere,⁹ considers charge injection from the metal into the organic by thermionic emission and a backflowing interface recombination, which is the time-reversed process of thermionic emission. Charge transport is described by time-dependent continuity equations, with field-dependent carrier mobilities and a drift–diffusion form for the current coupled to Poisson's equation. Carrier recombination is bimolecular with a Langevin

^{a)}Electronic mail: crone@lanl.gov

^{b)}Present address: Intel Corporation, Hillsboro, OR 97124-6497.

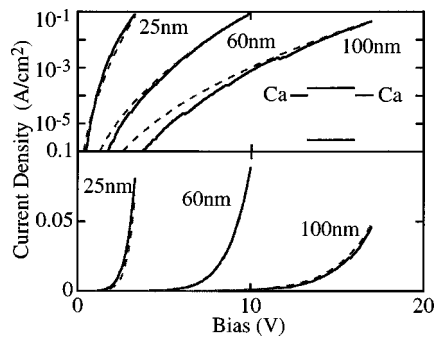


FIG. 1. Log-linear (upper panel) and linear-linear (lower panel) current density vs applied voltage bias for single-layer electron-only Ca/Ca devices with polymer film thicknesses of 25, 60, and 100 nm. Solid lines are measured values; dashed lines are model results. The inset schematically illustrates the relative positions of the Fermi energy of the contacts and the electron and hole polaron energies in the polymer.

vin form for the kinetic coefficient. Most of the input parameters required by the model can be measured directly. Capacitance measurements insure that the devices are fully depleted, and that device current is due to injected charge. The device thickness is measured by a Dektak profilometer and the Schottky energy barriers to injection, and hence, the built-in potential for a given choice of contacts, were determined in Ref. 10. Time-of-flight (TOF) measurements on organic materials have found a strongly field-dependent carrier mobility that can be parametrized by the form $\mu = \mu_0 \exp\sqrt{E/E_0}$.^{11,12} This form has also been derived theoretically for conduction through a spatially correlated Gaussian density of states (DOS).¹³ An alternative approach assumes a constant carrier mobility and introduces the DOS through a distribution of traps.^{14,15} The current voltage data for the single carrier structures is described by the device model using μ_0 and E_0 as fitting parameters. The device thickness and energy barriers are constrained to be within the error of their independently measured values. The mobility parameters extracted from the single carrier structures are then used to describe the bipolar devices. Device fabrication has been described previously.¹⁰

Figure 1 shows experimental and device model results for Ca/Ca electron-only structures with polymer thicknesses of 25, 60, and 100 nm. In these devices the Schottky energy barrier for electron injection is about 0.1 eV, leading to space-charge-limited current flow. The current depends on the bulk transport properties of the MEH-PPV layer. The fit electron mobility parameters are $\mu_{0e} = 5 \times 10^{-12}$ cm²/V s and $E_{0e} = 10^4$ V/cm for all thicknesses. This gives a mobility at 1 MV/cm of 10^{-7} cm²/V s. As seen from the semilog plot, the model describes the data over several orders of magnitude in current for device thicknesses of 25–100 nm. The model provides good agreement with the observed length scaling, which is not V^2/L^3 because of the field dependence of the carrier mobility.

Figure 2 shows experimental and device modeling results for Au/Al and Cu/Al hole only structures with polymer thicknesses of 100 nm. The Au/MEH-PPV contact has a small Schottky energy barrier for hole injection and is space-charge limited. The Cu/MEH-PPV contact has a ~ 0.7 eV Schottky energy barrier to hole injection and current flow is limited by the contact. The low current behavior of the Cu/Al

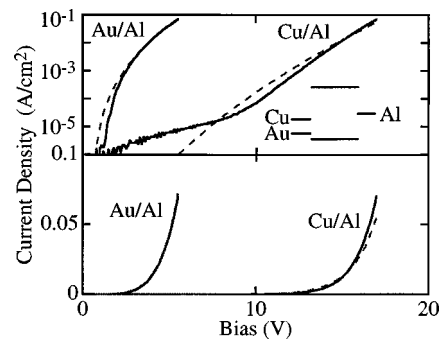


FIG. 2. Log-linear (upper panel) and linear-linear (lower panel) current density vs applied voltage bias for single-layer hole-only Au/Al and Cu/Al devices with polymer film thicknesses of 100 nm. Solid lines are measured values; dashed lines are model results. The inset schematically illustrates the relative positions of the Fermi energy of the contacts and the electron and hole polaron energies in the polymer.

device shows a leakage current, which varied from one device to another, and is most likely due to defects in the organic film. The fit hole mobility parameters are $\mu_{0h} = 5 \times 10^{-8}$ cm²/V s, and $E_{0e} = 1.3 \times 10^4$ V/cm, which gives a mobility at 1 MV/cm of 3×10^{-4} cm²/V s. The hole mobility obtained is consistent with those obtained by TOF measurements on a similar polymer.¹²

Figure 3 shows experimental and device model results for Pt/Ca devices with polymer thicknesses varying between 20 and 110 nm. The Pt and Ca contacts provide low-energy barriers for hole and electron injection, respectively. The current is limited by space charge and recombination and depends on the bulk properties of the polymer. Electron and hole mobilities determined from the fits to the single carrier devices are used without modification in the calculations; there are no fitting parameters. The device model agrees with the measured results for the Pt/Ca structures over several orders of magnitude in the current for device thicknesses ranging from 20 to 110 nm. The low current characteristics of the 40 nm device show a leakage current shoulder, which is not reproducible between different devices and is likely due to defects in the MEH-PPV film.

Figure 4 shows experimental and model results for Pt/Ca and Cu/Ca devices with polymer thicknesses of 100 and 80 nm, respectively. Pt and Ca are space-charge-limited hole

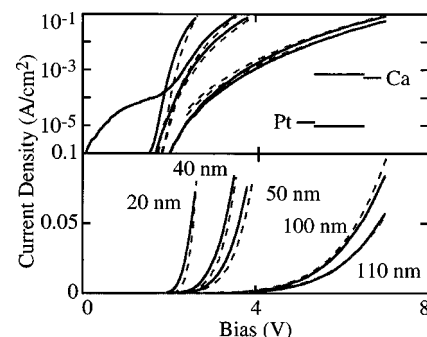


FIG. 3. Log-linear (upper panel) and linear-linear (lower panel) current density vs applied voltage bias for single-layer Pt/Ca devices with polymer film thicknesses of 20, 40, 50, 100, and 110 nm. Solid lines are measured values; dashed lines are model results. The inset schematically illustrates the relative positions of the Fermi energy of the contacts and the electron and hole polaron energies in the polymer.

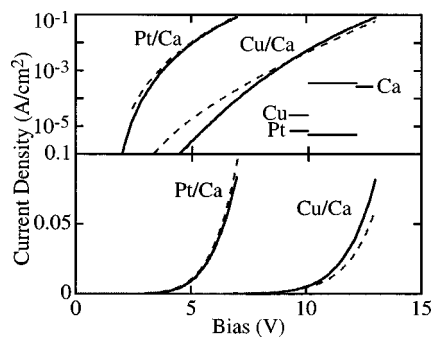


FIG. 4. Log-linear (upper panel) and linear-linear (lower panel) current density vs applied voltage bias for single-layer Pt/Ca and Cu/Ca devices with polymer film thicknesses of 100 and 80 nm, respectively. Solid lines are measured values; dashed lines are model results. The inset schematically illustrates the relative positions of the Fermi energy of the contacts and the electron and hole polaron energies in the polymer.

and electron contacts, respectively. The copper contact has a large barrier for hole injection and the hole current is contact limited in these structures. Because the hole mobility is larger than the electron mobility, most of the current is carried by holes in the Pt/Ca structures, but in the Cu/Ca structure, both electrons and holes carry a substantial fraction of the current due to the relatively large barrier to hole injection from the Cu contact. The electron and hole carrier mobilities used in the calculations are the same as those used for the single carrier devices; there are no fitting parameters. The model results agree with the data over several orders of magnitude in current for both types of devices.

We study the effect of recombination on device current-voltage characteristics by varying the value of the recombination kinetic coefficient used in the model. A decrease in the coefficient will decrease recombination and cause an increase in carrier densities, affecting the minority-carrier density more strongly. In devices like Pt/Ca, where the majority-carrier holes also dominate the current, reducing the kinetic coefficient by a factor of 10 results in less than a 1% increase of the modeled current at device current densities of the modeled current at device current densities of ~ 100 mA/cm². In devices like Cu/Ca, where electron and hole currents are comparable, reducing the kinetic coefficient by a factor of 10 results in a 25% increase of the modeled current at device current densities of ~ 60 mA/cm².

We have presented experimental and device model re-

sults for the current-voltage characteristics for single organic layer diodes. We considered three general types of structures: electron only devices, hole only devices, and bipolar devices with both electrons and holes. The current-voltage data for the single carrier structures is described by the device model using the material-dependent mobility factors μ_0 and E_0 as fitting parameters. The mobility parameters extracted from the single carrier structures are then used to describe the bipolar devices, with no additional fitting parameters. The device model described the experimental results for a thickness series of electron-only devices with space-charge-limited current and gave a good fit to the data over several orders of magnitude in current density. The device model described the experimental results of hole-only devices with Au/Al and Cu/Al contacts and gave a good fit over several orders of magnitude in current density. The model accurately describes bipolar devices, both for a thickness series of Pt/Ca structures, and devices with Cu/Ca contacts, without additional fitting parameters.

The authors would like to thank D. R. Brown for technical assistance. This work was funded in part by the Los Alamos National Laboratory LDRD program.

- ¹N. C. Greenham and R. H. Friend, *Solid State Phys.* **49**, 1 (1995).
- ²E. M. Conwell and M. W. Wu, *Appl. Phys. Lett.* **70**, 1876 (1997).
- ³P. W. M. Blom, M. J. M. de Jong, and S. Breedijk, *Appl. Phys. Lett.* **71**, 930 (1997).
- ⁴P. W. M. Blom, M. J. M. de Jong, and J. J. M. Vleggaar, *Appl. Phys. Lett.* **68**, 3308 (1996).
- ⁵I. D. Parker, *J. Appl. Phys.* **75**, 1656 (1994).
- ⁶M. Abkowitz, J. S. Facci, and M. Stolka, *Chem. Phys.* **177**, 783 (1993).
- ⁷B. K. Crone, I. H. Campbell, P. S. Davids, D. L. Smith, C. J. Neef, and J. P. Ferraris, *J. Appl. Phys.* (unpublished).
- ⁸I. H. Campbell, P. S. Davids, D. L. Smith, N. N. Barashkov, and J. P. Ferraris, *Appl. Phys. Lett.* **72**, 1863 (1998).
- ⁹P. S. Davids, I. H. Campbell, and D. L. Smith, *J. Appl. Phys.* **82**, 6319 (1997).
- ¹⁰I. H. Campbell, T. W. Hagler, D. L. Smith, and J. P. Ferraris, *Phys. Rev. Lett.* **76**, 1900 (1996).
- ¹¹M. A. Abkowitz, J. S. Facci, W. W. Limburg, and J. F. Yanus, *Phys. Rev. B* **46**, 6705 (1992).
- ¹²H. Meyer, D. Haarer, H. Naarmann, and H. H. Hörhold, *Phys. Rev. B* **52**, 2587 (1995).
- ¹³D. H. Dunlap, P. E. Parris, and V. M. Kenkre, *Phys. Rev. Lett.* **77**, 542 (1996).
- ¹⁴A. J. Campbell, D. D. C. Bradley, and D. G. Lidzey, *J. Appl. Phys.* **82**, 6326 (1997).
- ¹⁵P. E. Burrows, Z. Shen, V. Bulovic, D. M. McCarty, and S. R. Forrest, *J. Appl. Phys.* **79**, 7991 (1996).